ORIGINAL PAPER

On The Epidemic Spread Using Spline Tie-Decay Network Model

Chanon Thongprayoon*

Department of Statistics, Faculty of Science, Kasetsart University, Bangkok, Thailand

*Corresponding author: *thongprayoon.c@gmail.com*

Received: 26 June 2025 / Revised: 09 August 2025 / Accepted: 16 August 2025

Abstract. Standard epidemic compartmental models often overlook the evolving nature of inter-personal contact by assuming static interactions. To address this, we propose a deterministic SIR model driven by a spline tie-decay network, in which nodes represent individuals whose interactions (edge weights) gradually increase upon the arrivals of contact events under a cubic spline polynomial, followed by an exponential decay. This mechanism allows a flexible and realistic delay in how tie strength develops and fades over time. Here, the infection rate is dynamically computed as the sum of edge weights over the number of individuals squared, reflecting the state of the system without aggregating events into large time windows. In particular, this work highlights the importance of fine-grained temporal modeling in understanding and predicting disease spread dynamics.

Keywords: Temporal networks, Spline tie-decay networks, SIR dynamics

1. Introduction

In traditional epidemiological compartmental models, it is often the case to assume that contacts between individuals are either static or evolve in coarse ways over time (Barabási 2016). In reality, however, human interactions are time-dependent, which significantly affects the outcomes of disease spread. Over the past decades, temporal networks have become a popular tool for modeling such dynamics in a more realistic manner (Barrat et al. 2008; Masuda and Lambiotte 2020). Among these, tie-decay temporal network offers a means to model human contacts over time; tie-decay network models contact events as instantaneous increments of edge weights, followed by exponential decay in the absence of further contact (Ahmad et al. 2021). In this fashion, one captures the idea that the ties between pairs of individuals fade over time.

However, exponential decay alone does not realistically capture how contacts among pairs of individuals evolve, particularly, when the effects from delayed responses play a substantial role. For instance, certain social ties might not increase instantly after a contact, but rather gradually build up through time. This kind of behaviors is also found in epidemiological dynamics (Liu et al. 2020; Ma et al. 2004). To model such behaviors, we use an extension of the exponential tie-decay model, known as spline tie-decay model, which introduces a delayed response using clamped cubic spline kernels (Thongprayoon and Masuda 2025). This generalization enables more control over how edge weights form and fade, inducing richer contact dynamics.

To this end, we propose a deterministic SIR epidemic model in which the infection rate dynamically depends on the evolving spline-tie decay edge weights. That is, instead of having a fixed infection parameter, our model adapts its infectious potential according to the real-time state of the contact network without resorting to coarse-grained temporal aggregation (Holme 2015).

2. Exponential tie-decay and spline tie-decay networks

In this section, we provide the background of the tie-decay temporal network model (Ahmad et al. 2021) as well as its extension, the spline tie-decay network model (Thongprayoon and Masuda 2025).

Considering a network of N nodes, the exponential tie-decay network (or the tie-decay network) is a temporal network, in which the

edge weight exponentially decays over time (with a rate $\alpha > 0$) in the absence of event arrivals; otherwise, the edge weight instantaneously increases by 1 (Ahmad et al. 2021). Here, we assume that the input data set is a sequence of time-stamped contact events among edges. Given a pair of nodes i, j in the network, we denote by $\tilde{t}_l$ the time that l th event occurs on the edge $\{i, j\}$. Let $\tilde{b}_{ij}$ be the edge weight between the nodes i and j at time t, we then express $\tilde{b}_{ij}$ as follows:

$$\tilde{b}_{ij}(t) = \sum_{l\in\mathbb{N}} e^{-\alpha(t-\tilde{t}_l)} H(t-\tilde{t}_l) \qquad (1)$$

where H represents the Heaviside step function (Ahmad et al. 2021). In this work, one may regard an event arrivals in the network as a sequence of quadruplets $\{(i, j, \tilde{t}_l, \Delta_l): l \in \mathbb{N}\}$ which, for each l, $(i, j, \tilde{t}_l, \Delta_l)$ means an event occurs on the nodes i and j at time $\tilde{t}_l$ with the duration Δ_l (Masuda and Lambiotte 2020). Nevertheless, in many scenarios, the duration Δ_l is much smaller than the inter-event time, so one may ignore the duration of each event (Masuda and Lambiotte 2020). Therefore, the event arrivals are now a sequence of triplets $\{(i, j, \tilde{t}_l, \Delta_l): l \in \mathbb{N}\}$. Note that we reserve $\tilde{t}_l$ to denote the l th time step where at least one event arrives in the entire network, without being specific to any edge's events.

To this end, we have given the necessary background of the exponential tie-decay temporal network, we then will move on to the spline tie-decay temporal network, an extension of the exponential tie-decay temporal network by incorporating a time delay response using the clamped cubic spline polynomial (Thongprayoon and Masuda 2025). First, we begin by introducing ϕ(t), defined as

$$\phi(t) = \begin{cases} f(t), & t \in [0, h] \\ ke^{-\alpha(t-h)}, & t \in (h, \infty) \end{cases} \qquad (2)$$

Here, $f(t)$ denotes a cubic spline polynomial and $h, k > 0$ are parameters; moreover, f satisfies the following conditions: $f(0) = 0$, $f'(0) = 0$, $f(h) = k$, and $f'(h) = -k$ (Thongprayoon and Masuda 2025). Note that $'$ denotes the derivative with respect to time t, i.e. $\frac{d}{dt}$. With these imposed conditions on f, one expresses f in terms of the parameters α, h, k as follows:

$$f(t) = \left(-\frac{\alpha k}{h^2} - \frac{2k}{h^3}\right) t^3 + \left(\frac{3k}{h^2} + \frac{\alpha k}{h}\right) t^2 \qquad (3)$$

for all t ≥ 0 (Thongprayoon and Masuda 2025).

Finally, we denote by $b_{ij}(t)$ the edge weight between the nodes i, j in the spline tie-decay network. We then mathematically express the spline tie-decay edge weight as

$$b_{ij}(t) = \sum_{l:\tilde{t}_l \le t} \phi(t - \tilde{t}_l). \qquad (4)$$

3. Spline tie-decay epidemic spread via ordinary differential equations

In this section, we introduce an SIR model with a time-dependent infectious rate using the spline tie-decay edge weight.

3.1 The proposed SIR model

SIR model is a compartmental model for simulating epidemic spread where each node (or individual) either belongs to the susceptible compartment (S), the infectious compartment (I), or the recovered compartment (R) (Newman 2018). One uses differential equations expression of the model as follows.

$$\frac{dS}{dt} = -\beta SI$$

$$\frac{dI}{dt} = \beta SI - \gamma I$$

$$\frac{dR}{dt} = \gamma I, \qquad (5)$$

where $S(t) + I(t) + R(t) = N$, $\beta(> 0)$ denotes the infection rate and $\gamma(> 0)$ denotes the recovery rate. In our work, instead of

having a constant infection rate, we allow β to depend on time as shown in the following:

$$\beta(t) = \frac{\sum_{\{l:t_l \le t\}} \eta(t_l)\phi(t-t_l)}{N^2} \quad (6)$$

where $\eta(t_l)$ is the number of events arriving in the entire network at time t_l. Therefore, substituting (6) into (5) yields us the proposed deterministic SIR model.

3.2 Data and simulation method

The data set, referred to as Primary School, is a temporal contact network recorded from students and teachers in a primary school in Lyon, France over two days: 1/10/2009 and 2/10/2009 (Gemmetto et al. 2014; Stelé et al. 2011). In other words, it is an empirical data set of time-stamped events representing contacts between pairs of individuals and is provided by SocioPatterns (URL:https://www.sociopatterns.org). The data set contains the time-stamped contact events from 08:45 to 17:20 on the first day and from 08:30 to 17:05 on the second day. On each day, there are three breaks granting students to interact with peers in other classes. Such breaks are the morning break which begins at 10:30 and lasts for 20-25 minutes, the lunch break between 12:00 and 14:00, and the afternoon break which begins at 15:30 and lasts for 20-25 minutes.

Over both days, there are 242 individuals and 125,773 time-stamped contact events whereas there are 236 individuals and 60,623 (time-stamped) contact events on the first day. In our work, we only use the data on the first day. This is because the time period between the end of the first day and the beginning of the second day lets all the infectious nodes recover before the second day commences.

Like the previous study (Thongprayoon and Masuda 2025), we set $\alpha = 10^{-2}$ and we impose that the area under the curve in (2) is 1. The latter property enables us to express the parameter k in terms of α and h as shown in the following (Thongprayoon and Masuda 2025):

$$k = \frac{12\alpha}{12\alpha^2h^2+6\alpha h+12} \quad (7)$$

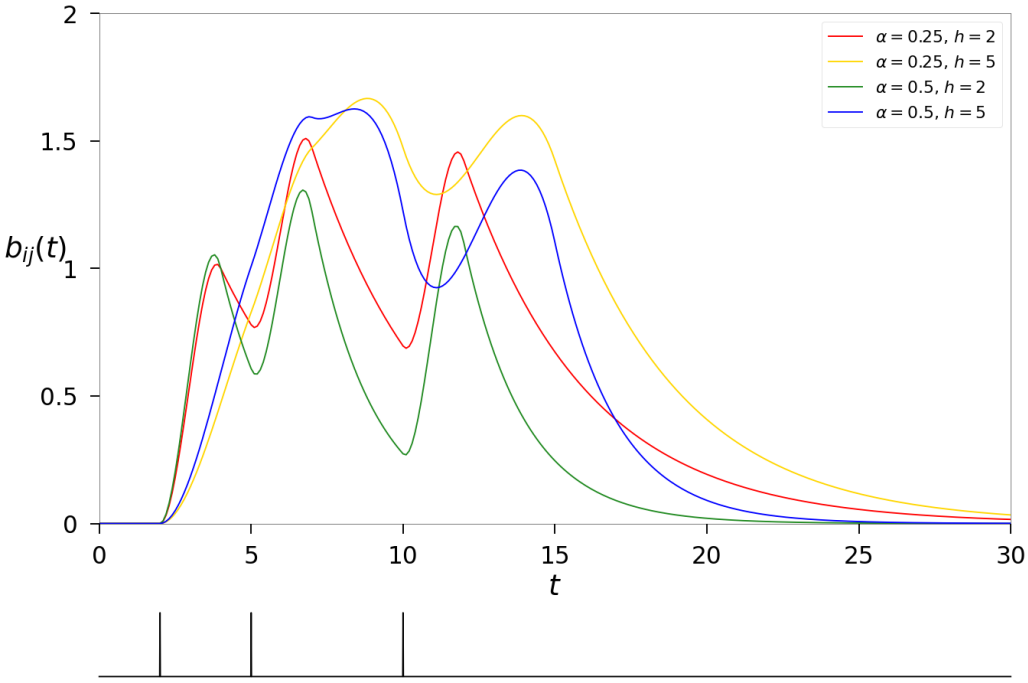

Figure 1. Time courses of the edge weight in spline tie-decay network. The vertical stubs under the plot represent the time of input events on the edge as follows: $\tilde{t}_1 = 2, \tilde{t}_2 = 5$ and $\tilde{t}_3 = 10$. We set $k = 1$ across all four combinations of $\alpha \in \{0.25, 0.5\}$ and $h \in \{2,5\}$.

To numerically simulate the epidemic dynamics, we apply Euler's method to (5) where we substitute the constant infection rate β with the time-dependent infection rate $\beta(t)$ defined on (6). Similar to the stochastic SIR simulations in (Thongprayoon and Masuda 2025), we advance each step of Euler's method with a time step of 2 seconds, which is one tenth of the time resolution of Primary School data set (20 seconds). At the beginning of each simulation, we set the number of infectious individuals to 1 and the remaining individuals are susceptible.

Moreover, previous studies show that the behaviors of the Primary School temporal network across two days are similar. Therefore, we only show the simulations on Day 1 of the network (Masuda and Holme 2019; Thongprayoon et al. 2023).

4. Numerical simulations

We show in Figure 2 the number of individuals in each compartment (see such numbers in Figures 2(a) for S, 2(b) for I, 2(c) for R), and the ratio $\frac{\beta(t)}{\gamma}$ (see Figure 2(d)), all plotted against time t, where different colors represent different h values. Here, we vary $h = 10, 400, 1000, 2000,$ and 3000. Together with $\alpha = 10^{-2}$, (7) implies that. $k \approx 9.52 \times 10^{-3}, 2.31 \times 10^{-3}, 6.98 \times 10^{-4}, 2.26 \times 10^{-4},$ and 1.10×10^{-4}, respectively. We set the recovery rate $\gamma = 5 \times 10^{-4}$, which is consistent with previous work in (Thongprayoon and Masuda 2025).

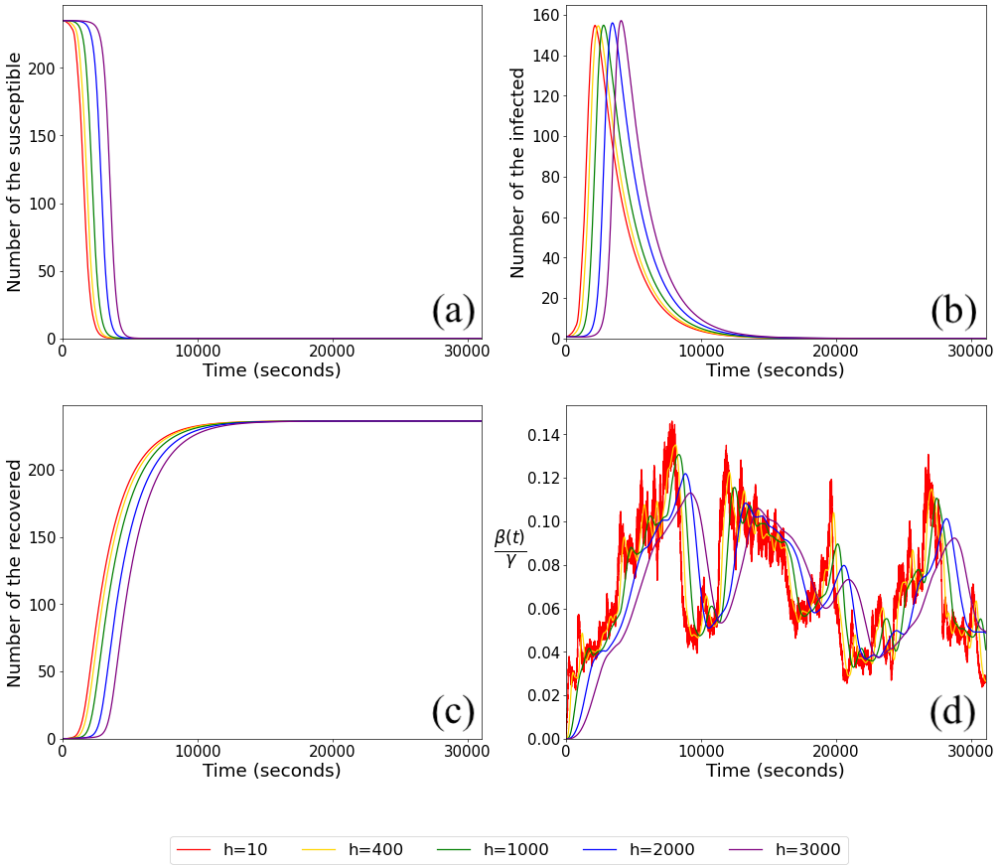

Figure 2. SIR dynamics on Day 1 of Primary School data set with the recovery rate $\gamma = 5 \times 10^{-4}$. (a) The number of individuals in the susceptible compartment. (b) The number of individuals in the infectious compartment. (c) The number of individuals in the recovered compartment. (d) The ratio between the (time-dependent) infection rate $\beta(t)$ and the recovery rate γ.

Given the result in Figure 2(a), we observe that the number of individuals in the susceptible compartment decreases monotonically with respect to the parameter h. That is, the smaller the h value is, the faster the decrement becomes. The result agrees with Figures 2(b) and 2(c) in that the number of infectious individuals reaches its peak faster when h is smaller and the number of recovered individuals reaches its plateau faster when h is smaller. Considering the early stage of the dynamics, we suggest that the aforementioned outcome arises because a smaller time delay parameter h increases the value of the infection rate $\beta(t)$ faster than that associated with a longer time delay, as evidenced by Figure 2(d). Lastly, because recovery rate γ is a constant, it does not affect the monotonicity of the individuals in each compartment. We confirm this statement with Figure 3, displaying the number of individuals in each compartment and the ratio $\frac{\beta(t)}{\gamma}$, where we set $\gamma = 10^{-4}$. One observes that the monotonicity of the dynamics in Figures 3(a), 3(b), and 3(c) follows that of Figures 2(a), 2(b), and 2(c), respectively. Similar to Figure 2(d), considering the early stage of the dynamics, the value $\frac{\beta(t)}{\gamma}$ in Figure 3(d) is higher when h is smaller. Overall, the simulations in Figures 2 and 3 align with the data set's behavior because, as time progresses, more students interact with their peers, leading to an increase in the number of the infectious compartment.

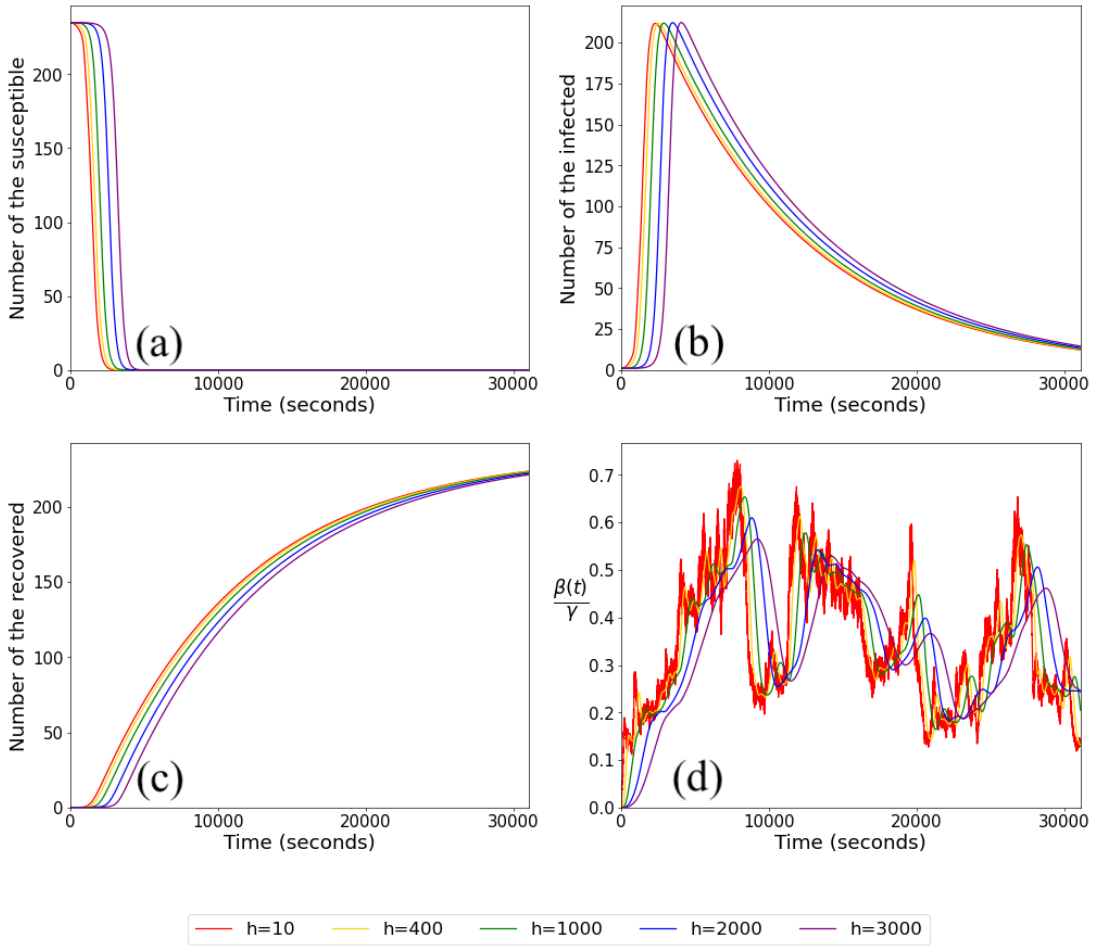

Figure 3. SIR dynamics on Day 1 of Primary School data set with the recovery rate $\gamma = 10^{-4}$. (a) The number of individuals in the susceptible compartment. (b) The number of individuals in the infectious compartment. (c) The number of individuals in the recovered compartment. (d) The ratio between the (time-dependent) infection rate $\beta(t)$ and the recovery rate γ.

6. Discussion

As we have presented our findings in this article; nevertheless, there is a direction for future investigations: the effect of the time delay in long terms, for instance. One observes that there are durations (when t is approximately more than 10^4) in which the fraction $\frac{\beta(t)}{\gamma}$ associated with larger h values are higher than those associated with smaller h, owing it to the aggregation of contact events because the larger time delay slows down the edge weight from entering the exponential decay part. This property could play an important role in the dynamics in other epidemic models such as the SIS model, where we wish to establish long term equilibriums of the individuals in the susceptible and the infectious compartments.

All in all, we propose in this article a variation of the SIR model in which we consider a time-dependent infection rate, constructed by averaging all the edge weights of the spline tie-decay network model (Thongprayoon and Masuda 2025). We then observe that when one varies the time-delay parameter h, there is a monotonic tendency with the number of individuals in each compartment plotted against time. This outcome, especially with the number of recovered individuals, is consistent with the stochastic SIR dynamics, presented in Thongprayoon and Masuda 2025, with one different characteristic: the final number of recovered individuals. We suspect that this difference is naturally caused by the distinction of the simulation methods, especially the difference between a deterministic-based and a stochastic-based methods.

References

Ahmad W, Porter M, Beguerisse-Díaz M (2021) Tie-decay networks in continuous time and eigenvector-based centralities. In: IEEE Transactions on Network Science and Engineering, IEEE, pp 1759–1771.

Barabási A-L (2016) Network science. In: Network Science, Cambridge University Press, Cambridge, UK.

Barrat A, Barthelemy M, Vespignani A (2008) Dynamical processes on complex networks. In: Dynamical Processes on Complex Networks, Cambridge University Press, Cambridge, UK.

Gemmetto V, Barrat A, Cattuto C (2014) Mitigation of infectious disease at school: targeted class closure vs school closure. In: BMC Infectious Diseases, BioMed Central, 14:695.

Holme P (2015) Modern temporal network theory: a colloquium. In: European Physical Journal B, Springer, 88:1–30.

Liu Z, Magal P, Seydi O, Webb G (2020) A COVID-19 epidemic model with latency period. In: Infectious Disease Modelling, Elsevier, 5:323–337.

Ma W, Song M, Takeuchi Y (2004) Global stability of an SIR epidemic model with time delay. In: Applied Mathematics Letters, Elsevier, 17:1141–1145.

Masuda N, Holme P (2019) Detecting sequences of system states in temporal networks. In: Scientific Reports, Nature, 9:1–11.

Masuda N, Lambiotte R (2020) A guide to temporal networks. In: A Guide to Temporal Networks, 2nd edition, World Scientific, Singapore.

Newman M (2018) Networks. In: Networks, Oxford University Press, Oxford, UK.

Stehlé J, Voirin N, Barrat A, Cattuto C, Isella L, Pinton JF, Quaggiotto M, Van den Broeck W, Régis C, Lina B, et al. (2011) High-resolution measurements of face-to-face contact patterns in a primary school. In: PLoS ONE, Public Library of Science, 6:e23176.

Thongprayoon C, Livi L, Masuda N (2023) Embedding and trajectories of temporal networks. In: IEEE Access, IEEE, 11:41426–41443.

Thongprayoon C, Masuda N (2025) Spline tie-decay temporal networks. In: Journal of Computational Science, Elsevier, 88:102591.